

Activation of Apoptosis and Caspase-3 in Zebrafish Early Gastrulae

Javier F. Negrón[†] and Richard A. Lockshin^{*}

Nonmammalian vertebrate embryos do not manifest apoptosis before gastrulation, and it has been suggested that their cells are inhibited from undergoing apoptosis. To study this interesting possibility, the zebrafish (*Danio rerio*) embryo is an excellent model. However, the appearance of apoptosis varies among species, and many components of cell death are not highly conserved. To undertake the larger investigation, we first need to document by several criteria that cell death in the zebrafish embryo is apoptotic. Exposure of gastrulating germ-ring stage embryos to cycloheximide or staurosporine elicits an arrest in development and cell death within 8 hr. Caspase-3 activity increases, followed by translocation of phosphatidylserine, loss of cell–cell adhesion, cleavage of poly (ADP-ribose) polymerase, terminal deoxynucleotidyl transferase-mediated dNTP-fluorescein nick end labeling (TUNEL)-positive nuclei, internucleosomal DNA fragmentation, chromatin condensation and margination, and blebbing of the nuclear membrane. Thus, by many criteria, cell death in zebrafish is apoptotic; many of the markers of apoptosis found in mammals are conserved in zebrafish; and post-midblastula transition embryos have the capacity to activate a caspase-dependent apoptotic response well before naturally occurring programmed cell death is seen. *Developmental Dynamics* 231:161–170, 2004. © 2004 Wiley-Liss, Inc.

Key words: apoptosis; embryo; zebrafish; *Danio*; caspase-3; cycloheximide; TUNEL; gastrulation

Received 29 January 2004; Revised 3 April 2004; Accepted 6 April 2004

INTRODUCTION

A cell's decision to undergo apoptosis is an important event in development, homeostasis, and pathology. How this decision is reached is unclear, as is the distinction between committing to apoptosis or to another form of cell death. For studies of such questions, cell death in embryos is a useful model. In most embryos, other than those of mammals, there is no cell death before the maternal-zygotic transition (MZT, the stage during which protein synthesis directed by maternal message gives way to that directed by zygotic

genes, typically near the 10th division in most embryos) and, indeed, cells in many cleavage-stage embryos, including starfish (Yüce and Sadler, 2001) and *Xenopus*, are reputed to be incapable of undergoing apoptosis (Hensey and Gautier, 1997, 1999; Ikegami et al., 1999; Mizoguchi et al., 2000). The question, therefore, arises as to whether they lack the machinery of apoptosis or apoptosis is actively suppressed in these embryos.

The zebrafish (*Danio rerio*) embryo can serve well to investigate these questions. It is a vertebrate for which

direct comparisons can be made to other vertebrates, including mammals, and its genome is being completely sequenced. However, cell death can occur in different forms such as autophagy, necrosis, and other variants, and genes associated with apoptosis show variable levels of evolutionary conservation (Lockshin and Zakeri, 2002, 2003; Levraud et al., 2003). Indeed, in several examples, cell death has been severely underestimated, because dying cells did not display a marker of apoptosis probed in the experiment (Oppenheim et al., 2001). Thus,

Department of Biological Sciences, St. John's University, Jamaica, New York

Grant sponsor: National Institutes of Health; Grant number: R15GM/AAG57614; Grant number: R25 GM56821; Grant sponsor: US Department of Education; Grant number: GAANN #P200A9801 25-99.

[†]Dr. Negrón's current address is Precept Medical Communications, Berkeley Heights, NJ 07922.

^{*}Correspondence to: Richard A. Lockshin, Department of Biological Sciences, St. John's University, Jamaica, New York, 11439. E-mail: lockshin@stjohns.edu

DOI 10.1002/dvdy.20124

Published online 1 July 2004 in Wiley InterScience (www.interscience.wiley.com).

before one can ask the major questions concerning mechanisms, one must first verify that cell death in the zebrafish embryo is apoptotic by recognizable criteria. In this first publication, we provoke cell death in zebrafish embryos and evaluate the form of cell death by several means, to demonstrate that this death is apoptotic by all usual criteria. In a subsequent publication, we will examine the question of the inability of pre-MZT cells to undergo apoptosis.

RESULTS

For all experiments, germ-ring stage (~3 hr) embryos were exposed to 100 $\mu\text{g}/\text{ml}$ cycloheximide for up to 8 hr. This exposure causes rapid synchronous cell death approximately 7 hr later. Lower levels of cycloheximide (CHX; we evaluated 1–500 $\mu\text{g}/\text{ml}$) caused cell death but with greater delay and scatter. Given the rapid development of the embryo, we elected to evaluate cell death at the 100 $\mu\text{g}/\text{ml}$ concentration used by many researchers. Similar results, although slightly delayed and less synchronous, are obtained with camptothecin, a topoisomerase I inhibitor, or nocodazole, a microtubule destabilizer (Ikegami et al., 1997a,b, 1999) and confirmed by us (data not shown).

CHX Treatment Forces a Rapid Arrest in Development

The first obvious effect of CHX treatment in germ-ring stage zebrafish embryos is the abrupt cessation of development (Fig. 1A). CHX-treated embryos progress to approximately the shield stage after 1 hr. Thereafter, the embryos undergo sequential deterioration: 2nd hr—there is an obvious arrest in stage progression, changes in cell adhesion and changes in embryonic morphology, and the germ-ring margin begins to disappear; 3rd hr—embryos display extensive retraction toward the animal pole, possibly due to embryo contraction and loss of cell adhesion to the vegetal pole. By the 4th hr, the animal pole begins to detach from the vegetal pole, indicating extensive loss in cell-cell adhesion; 5th hr—the animal pole cells begin to display extensive loss of cell-cell

contact; 6th hr—the cytoplasm of most of the animal pole cells has opacified. Death of the embryo is obvious by the 7th hr as most animal pole cells have ruptured. Untreated control embryos develop as expected (Fig. 1B).

If these deaths are apoptotic, CHX-treated germ-ring stage embryos contain constitutive cell death machinery that responds to the protein synthesis inhibitor. The origin of this machinery is presumptively zygotic in these post-MZT animals. In *Xenopus* embryos, CHX inhibits cyclin synthesis at the two-cell stage and causes an arrest in cell division within 1 hr of treatment. However, the embryos did not die until a time when they would normally be gastrulating (Hensey and Gautier, 1997), suggesting to these authors that the

apoptotic machinery was inoperative.

Populations of CHX-Treated Embryos Die in a Consistent Manner

Populations of embryos at the germ-ring stage were incubated in 100 $\mu\text{g}/\text{ml}$ CHX for up to 8 hr. The death described above was highly reproducible, with 10% of the embryos dying by the 5th hr, another 20% dying in the 6th hr, and the rest dying in the 7th and 8th hr (Fig. 2A). All populations studied appear to have similar gross morphologies seen in deaths induced by other agents used against zebrafish and *Xenopus* embryos (Hensey and Gautier, 1997; Ikegami et al., 1997a,b, 1999).

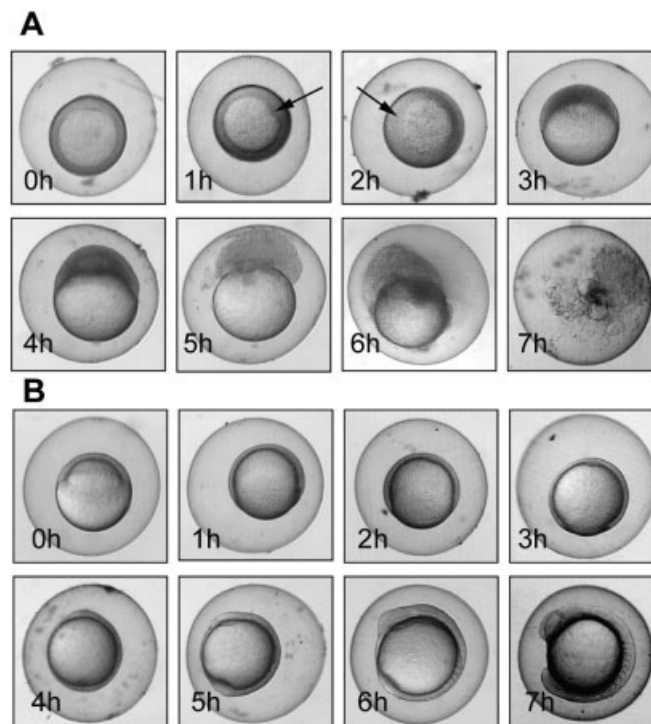


Fig. 1. Sequential digital recording of synchronously dying cycloheximide-treated germ-ring stage embryos. Germ-ring stage embryos were incubated in embryo rearing medium with 100 $\mu\text{g}/\text{ml}$ of cycloheximide. **A:** The 0 hr–7 hr (h) of exposure to cycloheximide beginning at germ-ring stage. **B:** The 0–7 are untreated control embryos. **A:** At 1 hr, germ-ring stage embryo shows signs of developmental retardation at the shield stage. The arrow points to the embryonic shield. At 2 hr, changes in cell adhesion and embryonic morphology are seen and the sharp germ-ring margin begins to disappear (arrow). By 3 hr, the embryo retreats toward the animal pole. At 4 hr, the animal pole of the embryo begins to detach from the vegetal pole. By 5 hr, the animal pole begins to display extensive loss of cell-cell contact; by 6 hr, the cytoplasm of most of the cells has darkened (denatured) in the animal pole, and by 7 hr, most if not all of the cells in the animal pole have lysed. **B:** Panels 0–7h display normal developmental progression of untreated control embryos. All magnifications are $\times 52.5$.

Germ-Ring Stage Embryos Maintain an Intact Plasma Membrane Until Late in the Death Process

One of the features distinguishing dead from live cells is the loss of transport function and often even the loss of the structural integrity of the plasma membrane. Acridine orange (AO) exhibits metachromatic fluorescence that is sensitive to DNA conformation, making it useful for detecting apoptotic cells (Darzynkiewicz et al., 1994). AO is a cell-permeant nucleic acid intercalating dye that emits green fluorescence when bound to dsDNA and red fluorescence when bound to ssDNA or RNA. Because the intact membrane of live cells excludes charged dyes such as propidium iodide (PI), short incubation with this dye results in selective labeling of dead cells, while live cells show minimal uptake (Darzynkiewicz et al., 1992). Viewed by fluorescence microscopy, live cells stain lightly with AO and exclude PI. Apoptotic cells stain heavily with AO due to the increased binding of AO to fragmented DNA. Both late apoptotic cells and necrotic cells allow PI to pass through the cell membrane staining the DNA red, indicating a loss of plasma membrane integrity.

Germ-ring stage embryos maintain cell membrane integrity until sudden cell lysis. Germ-ring stage untreated control embryos maintain plasma membrane integrity as displayed by the light AO and PI staining (Fig. 2A,C). CHX-treated germ-ring stage embryos exhibited intense AO staining (Fig. 2B), yet displayed light PI staining (Fig. 2D), indicating that plasma membrane integrity is maintained in both types of treated embryos until they rupture suddenly, consistent with apoptosis, followed by osmotic influx of water when the ion pumps finally collapse.

Nuclear and Chromatin Fragmentation Occurs During CHX Treatment

We used vital staining with the DNA binding dye Hoechst 33342 to analyze nuclear and chromatin morphology of CHX-treated germ-ring

stage embryos. During apoptosis, nuclear chromatin fragments into aggregates that stain brightly with fluorescent DNA dyes. Condensed nuclear chromatin gathers at the nuclear membrane and fragmentation of the nucleus then begins with the formation of micronuclei. Apoptotic and necrotic nuclei display different morphologies when viewed using electron microscopy. During necrotic cell death, mild clumping of nuclear chromatin can occur (Trump et al., 1981) but necrotic chromatin clumps do not significantly redistribute and the aggregates that form during necrosis do not bud to form discrete, membrane-bound fragments.

Nuclei in control germ-ring stage embryos displayed a general diffuse staining with Hoechst 33342 (Fig. 3A,C). Mitotic cells were also highly stained, with chromosomes clearly visible (Fig. 3E). CHX-treated germ-ring stage embryos displayed characteristic apoptotic nuclei and chromatin (Fig. 3B,D,F). Convolution of the nuclear membrane and the formation of chromatin clumps confirms that germ-ring stage embryos display classic apoptotic nuclear changes when exposed to CHX.

Extensive Genomic DNA Fragmentation Occurs During CHX Treatment

We assessed DNA fragmentation by terminal deoxynucleotidyl transferase (TdT)-mediated dNTP-fluorescein nick end labeling (TUNEL) assay (Gavrieli et al., 1992). During apoptosis, the nucleus undergoes extensive DNA fragmentation, the result of single- and double-strand breaks generated by caspase-activated DNase (CAD; Enari et al., 1998). The free 3'-OH groups are labeled (Gavrieli et al., 1992) by the incorporation of fluorescein conjugated deoxynucleotides at the sites of DNA breaks. In most instances, only apoptotic cells are labeled.

CHX-treated germ-ring stage embryos displayed extensive strand break formation and fragmentation in the genomic DNA of the embryos (Fig. 4A1). Untreated control germ-ring stage embryos displayed no TUNEL staining (Fig. 4A2). By this cri-

terion, germ-ring stage embryos have and use the machinery required for proper DNA fragmentation.

Extensive Internucleosomal DNA Fragmentation in the Death of Treated Germ-Ring Stage Embryos

A striking biochemical event in apoptosis is the internucleosomal cleavage of genomic DNA, initially producing 50- to 200-kb segments and fragments in multiples of approximately 185 bp (Wyllie, 1980; Oberhammer et al., 1993), as seen by agarose gel electrophoresis (Compton and Cidlowski, 1992). Caspase-3 initiates apoptotic DNA fragmentation by proteolytically cleaving DFF45/ICAD (DNA fragmentation factor-45 (DFF45)/inhibitor of CAD (ICAD)), which allows the release of active DFF40/CAD (Enari et al., 1998). DFF45/ICAD exists as a complex with a 40-kDa endonuclease termed DFF40/CAD that promotes apoptotic DNA fragmentation (Enari et al., 1998). CHX treatment of germ-ring stage embryos produces extensive laddering by the 2nd hr of treatment and continues to produce smaller oligonucleosomal fragments up to the 8th hr (Fig. 4B).

Pro-Caspase-3 Is Present and Can Be Activated in Treated Germ-Ring Stage Embryos

The active form of one or more caspases is required for the characteristic morphology associated with apoptosis. The regulation of caspase activity occurs predominantly at the level of proenzyme processing and maturation. Dormant caspase proenzymes are converted to catalytically competent heterodimeric proteases by cleavage at Asp-x bonds. Most of the changes of apoptosis can be attributed to caspase activity. CHX-treated germ-ring stage embryos activate caspase-3 beginning by the 2nd hr of treatment and reaching a peak by the 7th hr of incubation (Fig. 5A).

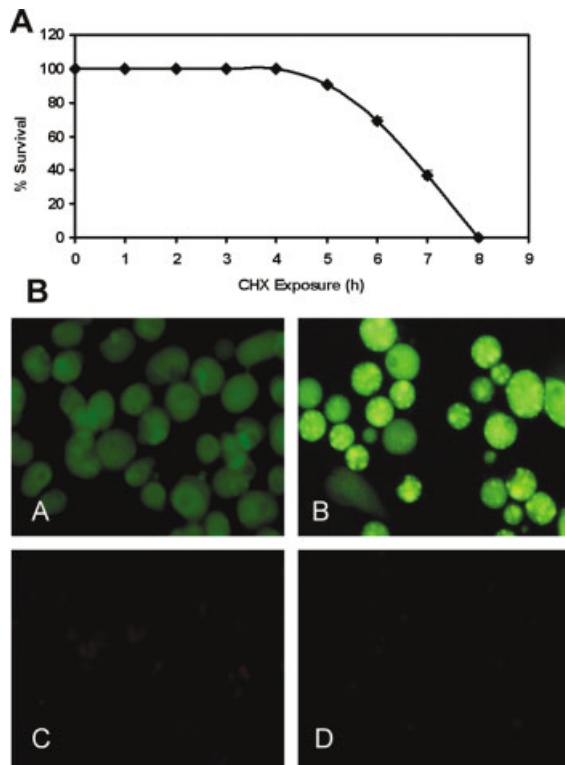


Fig. 2.

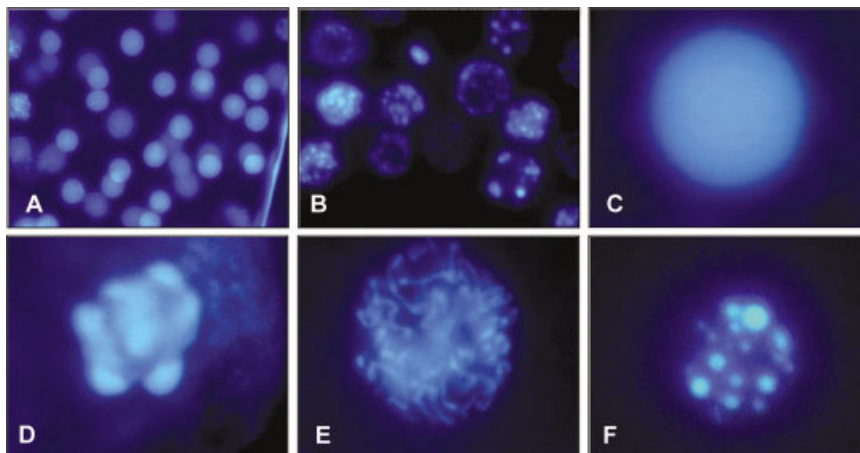


Fig. 3.

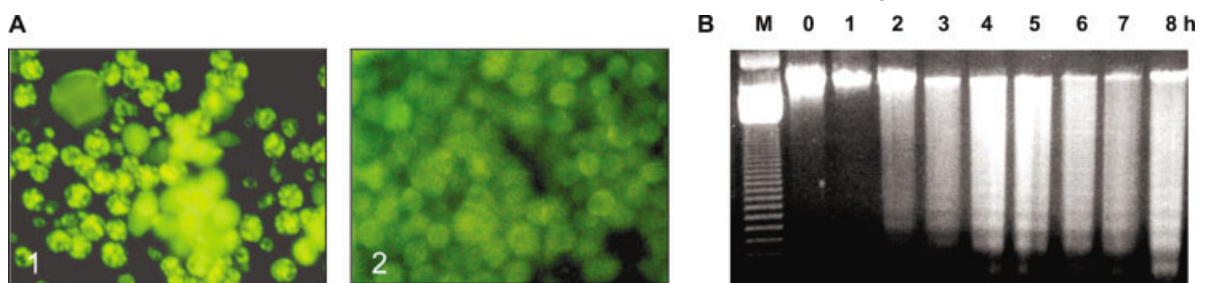


Fig. 4. Terminal deoxynucleotidyl transferase-mediated dNTP-fluorescein nick end labeling (TUNEL) labeling in germ-ring stage embryos after incubation with 100 $\mu\text{g}/\text{ml}$ of cycloheximide for 4 hr. A: (A1) Extensive TUNEL label is seen in germ-ring stage embryos exposed to cycloheximide. Chromatin condensation can also be seen in visibly apoptotic animal pole cells. (A2) Untreated control germ-ring stage embryos display only background levels. Original magnification, $\times 200$. B: Agarose gel electrophoresis analysis of internucleosomal DNA fragmentation in cycloheximide-treated embryos (60 embryos/lane). Germ-ring stage embryos exposed to cycloheximide display extensive internucleosomal DNA fragmentation beginning within 2 hr of exposure. M, molecular weight markers; 0–8, hours after beginning cycloheximide.

Fig. 2. A: Percentage survival curve for zebrafish germ-ring stage embryos, with death defined as $>50\%$ of the cells lysed in an embryo. For each experiment, 100 embryos were used, and the experiment was repeated three times. Cell death was induced as previously described. Embryos were counted, and dead embryos were removed at hourly intervals. B: (Upper) Treatment of germ-ring stage embryos with cycloheximide (CHX) caused embryonic death beginning at the 5th hr of treatment, equivalent to 11 hours postfertilization in untreated controls. By the 8th hr of treatment, all embryos were judged to be dead, a time corresponding to the early segmentation period in untreated control embryos. (Lower) Determination of embryonic viability by acridine orange (AO)/propidium iodide (PI), live/dead assay in CHX-treated 64-cell blastomeres and germ-ring stage embryos. Cell death was induced in zebrafish germ-ring stage embryos by treatment with 100 $\mu\text{g}/\text{ml}$ of CHX for 4 hr. Isolated animal poles were examined in embryo rearing medium (ERM) after incubation in ERM containing AO and PI. BA: Untreated control germ-ring stage embryos display light cytoplasmic staining with AO. BB: Cycloheximide-treated germ-ring stage embryos display extensive staining of the chromatin clumps with AO. BC, BD: Untreated control germ-ring stage embryos (BC) and CHX-treated germ-ring stage embryos (BD) exclude PI until the late stages of apoptosis. All magnifications are $\times 200$.

Fig. 3. Morphological analysis of nuclear fragmentation and chromatin condensation with Hoechst 33342 in cycloheximide (CHX)-treated germ-ring stage embryos. Animal poles from dechorionated, CHX-treated embryos were stained with Hoechst 33342 in embryo rearing medium. A, B: Untreated control germ-ring stage embryos (A) display normal HOE staining, whereas CHX-treated germ-ring stage embryos (B) display chromatin clumping morphology characteristic of apoptosis and formation of micronuclei. Original magnification, $\times 200$. C–E: Untreated control germ-ring embryo (C), compared with an apoptotic germ-ring stage nucleus (D) indicates extensive chromatin clumping and the generation of nuclear membrane convolutions in the apoptotic nucleus, whereas a prophase cell is easily recognizable (E). Original magnification, $\times 1,000$. F: A germ-ring stage cell that has many micronuclei a late event in apoptosis. Original magnification, $\times 400$.

Caspase-3 Is Dispersed Throughout the Cell During CHX Treatment

In humans, the caspase family consists of 14 proteolytic enzymes (caspases 1–14). The enzymes have in common similar cleavage specificities and amino acid sequences, and they are expressed as proenzymes. Caspase-3, the main effector caspase, is responsible for many of the morphological and biochemical cell changes that are the hallmark of apoptosis (Nicholson and Thornberry, 1997). In mouse liver, procaspase-3 is present in both cytosol and mitochondria. During Fas-induced apoptosis, active caspase-3 is confined primarily to the cytosol (Chandler et al., 1998).

Embryos were incubated with the synthetic fluorogenic caspase-3 peptide substrate Ac-Asp-Glu-Val-Asp-AFC (Ac-DEVD-AFC; CALBIO-CHEM, La Jolla, CA). Intact DEVD-AFC emits blue fluorescence (~400 nm), whereas after proteolytic cleavage of the DEVD substrate by caspase-3, the freed AFC fluorophore emits a yellow-green fluorescence (~505 nm).

Untreated control embryos display no visible indications of caspase-3 activity (Fig. 5B2). In CHX-treated apoptotic germ-ring stage animal pole cells, active caspase-3 was seen throughout the cell (Fig. 5B1). Thus, the active form of caspase-3 is found in extensive quantities throughout the cytoplasm. Because the concentration of CHX needed to induce synchronous apoptosis (100 $\mu\text{g/ml}$) substantially exceeds that necessary to inhibit protein synthesis (1 $\mu\text{g/ml}$), it appears that procaspase-3 is constitutively present and that processing of the zymogen causes its activation throughout the cytoplasm.

Poly(ADP-ribose) Polymerase Is Cleaved in the Dying Embryos

Cleavage of poly(ADP-ribose) polymerase (PARP) precludes the catalytic domain of PARP from being recruited to sites of DNA damage. At the onset of apoptosis, caspase-3 cleaves PARP and inhibition of this cleavage attenuates apoptosis (La-

zebnik et al., 1994; Nicholson et al., 1995). We confirmed by Western blot of PARP digestion that CHX-induced cell death in zebrafish early embryonic animal pole cells is apoptotic.

For zebrafish PARP, the sequence of neither the mRNA nor the protein is known. We chose commercial antibodies according to their specificity against the most highly conserved region of PARP. The antibody detected a PARP-like molecule of 70 kDa (as opposed to 116 kDa for mammalian PARP) that was present only in extracts negative for caspase-3. Extracts that were positive for caspase-3 activity displayed a second band, approximately 25 kDa, the presumptive caspase-3 cleavage product. Both bands are similar in size to PARP bands seen on Western blots of apoptotic *Xenopus* embryos (Hensley and Gautier, 1997). CHX-treated germ-ring stage embryos display significant PARP cleavage by 4 hr, and extensive PARP cleavage was seen after the 5th hr of treatment (Fig. 6A). The activation of caspase-3 leads to the cleavage of PARP and the formation of a smaller molecular weight band in addition to the intact PARP band. Thus, caspase-3 activation results in the formation of PARP cleavage products, a hallmark of apoptosis.

Phosphatidylserine Is Translocated in CHX-Treated Germ-Ring Stage Embryos

Phosphatidylserine is found almost exclusively on the inner leaflet of the cell membrane of healthy cells but is actively translocated to the outer leaflet during apoptosis (Martin et al., 1995) where it contributes to the "eat-me" signal of apoptotic fragments (Koopman et al., 1994). Translocation of phosphatidylserine to the outer leaflet of the cell membrane is an early marker of caspase-3 activation during apoptosis (Martin et al., 1995). Annexin V has a high affinity for phosphatidylserine. Phosphatidylserine localization was assayed with the Vybrant apoptosis assay kit, Alexa Fluor 488 conjugated to annexin V (Molecular Probes, Eugene, OR), which causes apoptotic cells to fluoresce green. If plasma mem-

brane integrity is lost, the nucleus fluoresces red from PI. Chromatin condensation, seen with blue 33342 fluorescence colocalizing with red PI, is an indicator of secondary necrosis.

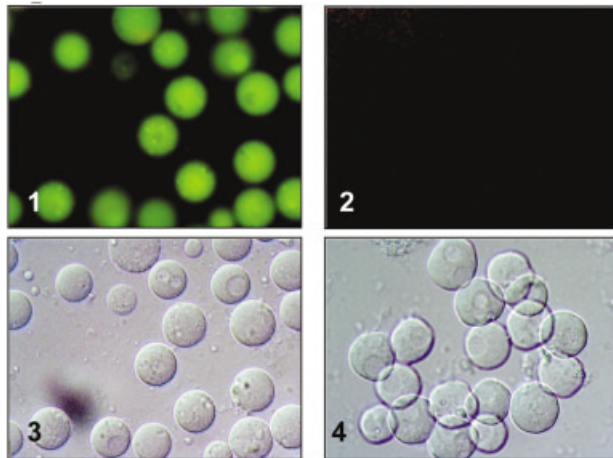
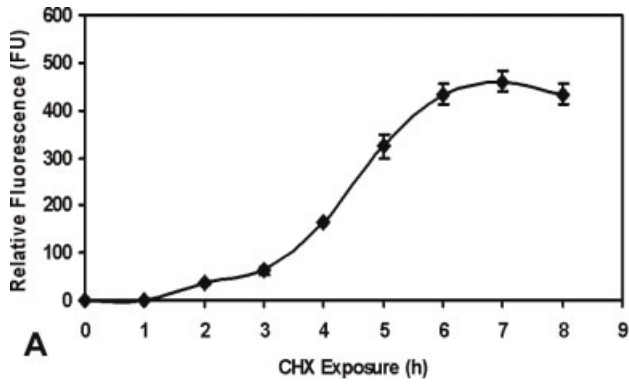
Untreated control embryos did not display any significant staining for phosphatidylserine (Fig. 6B). CHX-treated germ-ring stage embryos translocated phosphatidylserine to the outer leaflet of the plasma membrane. Thus, zebrafish embryos display also this marker for apoptosis.

Mitochondrial Transmembrane Potential Is Maintained in CHX-Treated Germ-Ring Stage Embryos

Disruption of $\Delta\Psi_m$, mitochondrial transmembrane potential, is often the immediate precursor to the activation of caspase 9. We used the DePsipher assay, which consists of a lipophilic cation that can be used as a mitochondrial activity marker, to analyze the mitochondrial transmembrane potential in CHX-treated germ-ring stage embryos. This indicator aggregates upon membrane polarization forming a focused orange-red fluorescent compound. If the potential is disturbed, the dye cannot access the transmembrane space and remains or reverts to its green monomeric form. Germ-ring stage embryos exposed to CHX display intact mitochondrial $\Delta\Psi_m$ as late as the 4th hr of treatment, as they do in untreated control embryos (Fig. 7). Thus, the mitochondrial $\Delta\Psi_m$ is maintained until late into apoptosis.

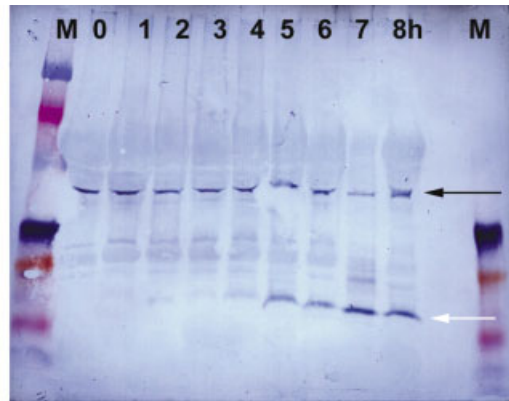
Extensive Changes in Nuclear Morphology Are Seen in CHX-Treated Germ-Ring Stage Embryos

The earliest and most obvious unequivocal morphological evidence of a classically apoptotic cell is nuclear. The first apoptotic nuclear change is the condensation of nuclear chromatin into aggregates that migrate to the nuclear membrane. Slight convolution of the nuclear membrane outline is evident just before budding of the nucleus

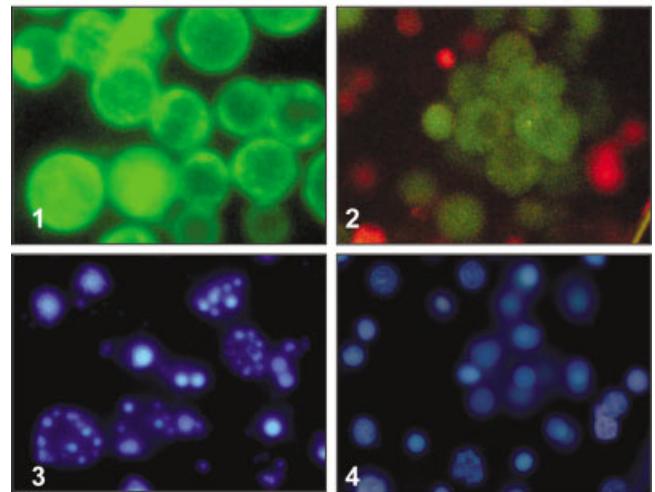


B

Fig. 5.



A



B

Fig. 6.

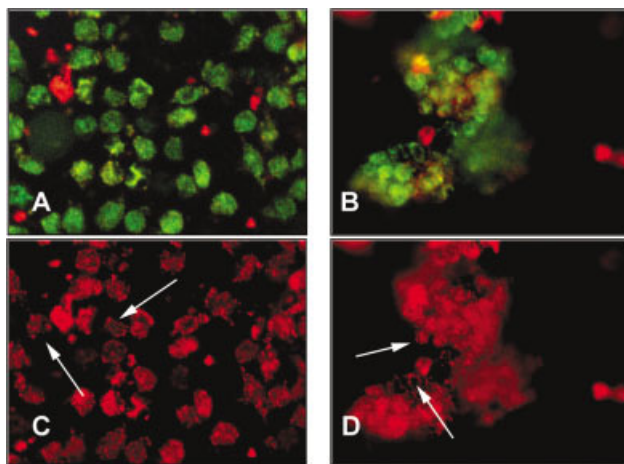


Fig. 7. Mitochondrial transmembrane potential in cycloheximide-treated germ-ring stage embryos. **A,B:** Monomeric form of DePsiher in cycloheximide-treated germ-ring stage embryonic cells (**A**) and in untreated control germ-ring stage embryonic cells (**B**). **C,D:** Cycloheximide-treated germ-ring stage embryos also display extensive amounts of red aggregate formation (arrows, **C**), indicative of healthy $\Delta\Psi_m$, as do untreated control germ-ring stage (arrows, **D**). Original magnification, $\times 200$.

occurs. Condensed chromatin gathers at the convolutions, and as the convolutions become extreme, budding of the nucleus begins, followed by cytoplasmic blebbing. The classic nuclear morphology seen during apoptosis is dependent on the presence of functional caspase-3 (Woo et al., 1998).

Germ-ring stage embryos display a classic apoptotic nucleus, complete with all landmarks. After 6 hr of CHX, we see extensive changes in nuclear morphology in many cell layers. The most common changes are margination of condensed chromatin, convolution of the nuclear membrane, and fragmentation of the nucleus. Untreated control embryos display light clumping of the chromatin and a lack of margination (Fig. 8). Thus, by nuclear morphology, CHX induces apoptosis in germ-ring stage embryos.

DISCUSSION

Several studies, including those on amphibian and zebrafish have argued whether or not an early embryo can manifest apoptosis. CHX is often used to induce apoptosis, and typically it is used at concentrations well above the approximately 1 $\mu\text{g/ml}$ needed to block protein syn-

Fig. 5. A: Caspase-3 activity in cycloheximide (CHX)-treated germ-ring stage embryos. Groups of 30 embryos were randomly removed from the population at hourly intervals up to 8 hr. Germ-ring stage embryos activate caspase-3 beginning 2–3 hr after beginning of CHX treatment and achieving massive activation by the 4th hr. Lower levels of CHX also activated caspase-3 but with greater delay and more scatter. Levels of caspase activity in controls remained at the negligible levels indicated at 0–1 hr. Because the control embryos continued to advance through gastrulation and early somite formation, the values were not included in the graph. **B:** The caspase-3 live cell enzyme assay detected extensive cytoplasmic caspase-3 activity. Enhanced AFC fluorescence visualized in CHX-treated animal pole cells, indicating (B1) activation of caspase-3 in the cytoplasm of untreated control zebrafish animal pole cells display no fluorescence, (B2) caspase-3 inactivity under normal conditions. B3, B4: Differential interference contrast microscopy images of the same cells. Original magnification, $\times 200$.

Fig. 6. Parameters of apoptosis in cycloheximide-exposed embryos. **A:** Extensive poly(ADP-ribose) polymerase (PARP) cleavage in germ-ring stage embryos exposed to cycloheximide. M, molecular weight markers; 0–8, hours after beginning of exposure. Intact PARP (black arrow at 70 kDa) can be seen in 0 hr untreated control zebrafish early embryos. Small amounts of cleaved PARP can be seen after the 1st hr of cycloheximide treatment, and extensive cleavage after the 4th hr of cycloheximide treatment (white arrow at approximately 25 kDa). Embryos permitted to continue development for 8 hr contained intact PARP with no fragments, as at 0 hr. **B:** Detection of annexin V binding in apoptotic zebrafish early embryonic cells. B1: Enhanced annexin V/Alexa Fluor 488 staining visualized in cycloheximide-treated embryos indicates a translocation of phosphatidylserine from the inner to the outer leaflet of the plasma membrane. B2: Untreated control zebrafish animal poles show weak fluorescence indicating normal cell membrane inner localization of phosphatidylserine. B3: Extensive chromatin condensation evident in cycloheximide-treated embryos after 4 hr perfusion. B4: Normal nuclear morphology is seen in untreated control embryos. Original magnification, $\times 400$.

thesis. Although rarely discussed, the mechanism by which it induces a synchronous and extensive apoptosis is distinct from its inhibition of protein synthesis but is not known. *Xenopus* embryos treated with CHX before the mid-blastula transition (MBT) undergo cell cycle arrest and show signs of apoptosis at stage 10.5, whereas embryos treated after the MBT undergo cell cycle arrest, but do not display signs of apoptosis until much later (Hensey and Gauthier, 1997). The first signs of apoptosis in these embryos are evident during neurulation at 15.5 hours postfertilization (hpf); many of these embryos survive up to 24 hpf, but development is abnormal (Hensey and Gauthier, 1997). However, Yabu et al. cloned zebrafish caspase-3, the major effector caspase involved in apoptosis and detected its message as early as the formation of the zygote (Yabu et al., 2001a). Because early embryos between the 4-cell and 1,024-cell stages had high levels of caspase-3 mRNA, these authors considered that the message was maternal. After gastrulation, zygotic housekeeping genes and caspase-3 were expressed (Yabu et al., 2001a). Normally developing embryos have only low levels of caspase-3 activity localized to individual cells that are apoptotic (Yabu et al., 2001b), but overexpression of zebrafish caspase-3-induced apoptosis and increased ceramide levels in zebrafish embryos (Yabu et al., 2001a).

Camptothecin (a topoisomerase I inhibitor) immediately arrests cell division in post-MBT zebrafish embryos, but the embryos remain alive until ~ 10 hr of age, when they rapidly die (Ikegami et al., 1997b, 1999). In response to an early, pregastrulation, treatment with camptothecin, apoptosis was induced at a time corresponding approximately to mid-gastrula stage in control embryos but not before this time (Ikegami et al., 1997b, 1999).

In our experiments, after CHX treatment, germ-ring stage zebrafish embryos displayed many of the characteristic changes associated with apoptosis. Under low magnification, the first visible sign of apoptosis that was seen was a loss of cell-cell adhesion in the animal pole

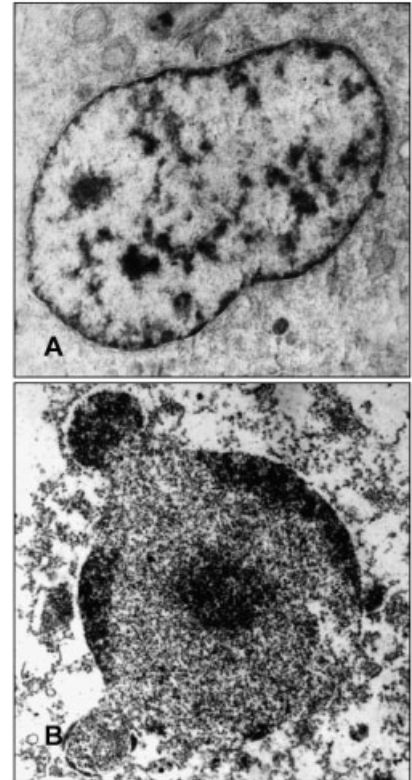


Fig. 8. Electron photomicrographs of cycloheximide-treated germ-ring stage nuclei. A is an untreated control; B was exposed to cycloheximide for 6 hr. **A:** Untreated control embryos display scattered patches of chromatin in the nuclei of normally developing animal pole cells. **B:** Experimental embryos display characteristic apoptotic morphology such as extensive chromatin condensation, margination, and budding of the nucleus. Original magnification, $\times 10,000$.

after 3 hr of treatment (Fig. 1A), interpreted, similar to most models of apoptosis, from *Caenorhabditis elegans* to *Homo sapiens*, as the loss of cell adhesion proteins from the cell surface. Once detachment occurs, bleb formation ensues, leading to the fragmentation of the cell. Animal pole cells from germ-ring stage embryos retain their plasma membrane integrity late in the cell death process, a further hallmark of apoptosis. PI is excluded from the cytosol and nucleus even though the nuclei of the animal pole cells contain highly condensed chromatin, stained by AO (Fig. 2B).

CHX-treated germ-ring stage embryos display many of the characteristic nuclear morphological changes associated with apopto-

sis. Extensive nucleoplasmic chromatin condensation was seen as early as the 2nd hr after CHX treatment (Fig. 3). Chromatin clumping, convolution of the nuclear membrane, margination of the condensed chromatin, and the fragmentation of the nucleus eventually ensued and were clearly visible in apoptotic animal pole cells (Fig. 8B). The genomic DNA of germ-ring stage embryos displayed extensive internucleosomal DNA fragmentation (presumably resulting from extensive cleavage of genomic DNA by CAD, which is activated as the result of caspase-3 activation) after only 2 hr of CHX treatment (Fig. 4B). Thus, by this criterion apoptosis can be induced in germ-ring stage embryos in less than 2 hr.

It is likely that most of the initial internucleosomal DNA fragmentation seen in this assay originated from the cells of the enveloping epithelial monolayer (EVL), but as time progressed, cells from the deep layer contributed to the intense fragmentation. TUNEL labeling of CHX-treated germ-ring stage embryos confirmed that the genomic DNA was extensively fragmented (Fig. 4A1).

Because transcripts for caspase-3 are present during early embryogenesis (Yabu et al., 2001a), we examined the functional activity of the enzyme, looking for signs of its function in situ, in cytosolic extracts, and through the use of Annexin V and immunoblot analysis for PARP cleavage. The importance of PARP cleavage during apoptosis in mammals was revealed when the insertion of an uncleavable PARP (lacking the caspase-3 cleavage site) into MEF cells caused a delay in cytoplasmic blebbing and nuclear disassembly during apoptosis (Oliver et al., 1998).

In situ evaluation demonstrated activated caspase-3, detected by the cleavage of Ac-DEVD-AFC, throughout the cytoplasm in CHX-treated germ-ring stage embryos (Fig. 5B). Cytosolic extracts could cleave the Ac-DEVD-AFC substrate after 2 hr of CHX (Fig. 5A). CHX-treated germ-ring stage embryos displayed extensive cleavage of PARP after 4 hr (Fig. 6A).

The translocation of phosphatidyl-

serine from the inner to the outer leaflet of the cell membrane is considered to be one of the earliest signs of caspase-3 activation (Martin et al., 1995). CHX-treated germ-ring stage embryos successfully translocate phosphatidylserine to the outer leaflet of the cell membrane (Fig. 6B), establishing for zebrafish this useful marker of apoptosis. Because phosphatidylserine translocation is only seen when caspase-3 is activated, the mechanism for its translocation appears to be conserved in zebrafish.

Thus, many of the markers of apoptosis found in mammals are conserved in zebrafish, and post-mid-blastula transition embryos have the capacity to activate a caspase-dependent apoptotic response well before naturally occurring programmed cell death is seen. The failure of cells to undergo apoptosis before neurulation, therefore, cannot be ascribed to an absence or blockage of apoptosis machinery. A following study will examine the acquisition of the apoptotic program.

EXPERIMENTAL PROCEDURES

Fish Stocks and Fish Aquaculture

Wild-type zebrafish embryos (*Danio rerio*) were used for all experiments. Aquaculture methods and staging were standard (Kimmel et al., 1995; Westerfield, 1998). Fish were maintained at 14 hr of light and 10 hr of dark per day. Each 40-liter tank held 30 fish at 28.5°C, and pH 7.0. The ratio of females to males was maintained at 2 to 1 for optimal embryo production.

To prevent scavenging of the eggs, 13-mm glass marbles were added to the tank bottoms. Fertilized eggs were collected by using a gravity-driven siphon. Siphoned tank water was discarded and replaced with fresh distilled water supplemented with 600 mg/l sea salts. Collected embryos were maintained in embryo rearing medium (ERM) at 28.5°C (Westerfield, 1998). At the germ-ring stage, embryos were isolated from the general population and grouped according to stage of development in fresh ERM.

CHX Treatment

Germ-ring stage embryos were placed in ERM containing CHX (100 µg/ml, Sigma-Aldrich). The concentration was chosen after preliminary evaluation of concentrations ranging from 1 to 500 µg/ml (see Results section). The embryos were held for up to 8 hr and were either immediately processed after treatment or groups of 15, 30, or 60 embryos were collected, snap frozen in crushed dry ice, and stored at -80°C.

Sequential Image Analysis

Cultured embryos were viewed with the Olympus SZH10 research stereo microscope and photographed with a NEC NC-15 CCD color camera at hourly intervals. All photographs were taken at ×52 magnification.

Staining: Acridine Orange/PI or Hoechst 33342

Stock AO and PI (Calbiochem) were prepared in ERM to a final working concentration of 100 µg/ml. Embryos were collected, washed in ERM, their chorions removed, animal poles isolated, and the animal poles placed into 100 µl of ERM with 1 µl of 100 µg/ml AO, and 1 µl of 100 µg/ml PI, and then incubated at room temperature for 15 min in the dark. Animal poles were washed with ERM, visualized by using a Nikon OPTIPHOT-2 fluorescence microscope with the appropriate filters, and photographed with a Pixera 120es digital microscope camera. Hoechst 33342 (bisbenzimidazole) was prepared and used similarly, at a working concentration of 100 µg/ml.

Genomic DNA Extraction

The genomic DNA extraction procedure was adapted from an established protocol (Gavrieli et al., 1992). Groups of 60 germ-ring stage embryos were thawed, 100 µl of high ethylenediaminetetraacetic acid lysis buffer was added, and the sample were homogenized. An additional 300 µl of lysis buffer was added, rehomogenized, and the preparation vortexed. A total of 200 µl of phenol:chloroform:isoamyl-alcohol (50:48:2) was

added, and the sample vortexed. The sample was then centrifuged for 5 min at 14,000 rpm at 4°C in a refrigerated microfuge and 350 μ l of upper aqueous phase was collected, and placed into a new centrifuge tube. A total of 200 μ l of chloroform:isoamyl alcohol (24:1) was added, and the tubes were vortexed and recentrifuged. A total of 250 μ l of the top aqueous phase was collected. A total of 100 μ l of 3 M sodium acetate was added, along with 800 μ l of ethanol, followed by Vortexing. The DNA was then precipitated at -20°C for 30 min. The sample was centrifuged for 10 min at 4°C. The supernatant was decanted and the pellet was dried at room temperature. The DNA was resuspended in 20 μ l of TE buffer. A total of 5 μ l of loading buffer was added to the sample, which was then loaded onto a 1% agarose gel and electrophoresed.

TUNEL Assay

The TUNEL assay was adapted from established protocols (Gavrieli et al., 1992; Yager et al., 1997; Chan and Yager, 1998), using the fluorescein-FragEL DNA fragmentation detection kit (Oncogene Research Products, San Diego, CA). Embryos were washed in TBS for 1 min at room temperature, fixed in 4% formaldehyde overnight at 4°C, washed 2 \times in TBS for 30 min at 4°C, dechorionated, incubated in 100 μ l of proteinase K solution in a hybridization chamber well for 20 min at room temperature, washed 2 \times for 10 min at room temperature, and then incubated in 100 μ l 1 \times TdT equilibration buffer for 30 min at room temperature. The buffer was then removed, 100 μ l of TdT labeling reaction mix was added, and the embryos were incubated for 90 min at 37°C in the dark. The reaction mix was then removed, and the embryos immersed in 100 μ l TBS for 5 min at room temperature. The sample was then rinsed with distilled H₂O and examined by fluorescence microscopy. As a positive control, embryos were initially exposed to DNase I (Sigma, 1 μ g/ml in PBS, 10 min at RT). The enzyme produced an intense TUNEL signal in all nuclei.

Fluorometric Enzyme Assay for Caspase-3 Activity

The assay used is an adaptation from the protocol of Mirkes and Little (2000). Groups of 30 frozen samples were used. A total of 510 μ l of fluorogenic lysis buffer was added, and the sample was homogenized. An additional 510 μ l of buffer was added, and the sample was rehomogenized. The sample was then Vortexed and centrifuged at 14,000 rpm for 20 min in a 4°C refrigerated microfuge. A total of 995 μ l of sample was then removed and placed into a cuvette. Five microliters of caspase-3 fluorogenic substrate (5 mg/ml, Bachem) was then added, and the sample was mixed. Fluorescence readings were taken every 15 min by using a 405-nm excitation filter and 515-nm emission filter. The readings were taken to 75 min, and because the responses were very linear, the 60 min reading was plotted.

DePsipher Mitochondrial Transmembrane Potential Assay

DePsipher (Trevigen, Gaithersburg, MD) solutions were prepared as indicated by the manufacturer. Live embryos were collected and washed in ERM, and their chorions removed. Animal poles were isolated and placed into 100 μ l of DePsipher reaction mixture on a printed diagnostic slide and incubated at 28.5°C for 15 min in the dark. They were then washed with ERM, covered with a coverslip, and visualized and photographed as above. Untreated control embryos were processed in the same manner.

Caspase-3 Live Cell Enzyme Assay

Animal pole cells were collected as above and placed into 100 μ l of ERM with 5 μ l of 5 mg/ml Ac-DEVD-AFC, 1 μ l of 100 μ g/ml PI, and 1 μ l of 100 μ g/ml H 33342, and then incubated at 28.5°C for 60 min in the dark and examined by fluorescence microscopy.

Annexin V Staining

Phosphatidylserine localization was assayed with the Vybrant apoptosis

assay kit, Alexa Fluor 488 conjugated to annexin V (Molecular Probes). Animal poles were collected as above and placed into 100 μ l of 1 \times annexin-binding buffer. One microliter of 100 μ g/ml PI, 1 μ l of 100 μ g/ml bisbenzimidazole H 33342, and 5 μ l Alexa Fluor 488 annexin V stock were added, and the preparations were incubated at room temperature for 15 min in the dark. They were washed with 1 \times annexin-binding buffer and visualized as above.

Western Blot and Electrophoresis

The Western blotting and electrophoresis procedure used was adapted from (Bollag et al., 1996) by using Kaleidoscope prestained standards (Bio-Rad Laboratories, Hercules, CA). Samples were directly applied to 4-15% Bio-Rad precast Ready gels, and a Bio-Rad Mini-PROTEAN II unit at 200 volts. Immediately after electrophoresis, the gels were overlaid with Bio-Rad Immun-Blot polyvinylidene difluoride (PVDF) membrane and blotted at 100 V for 90 min. The PVDF membranes were blocked by using 3% bovine serum albumin for 60 min. The gel was stained with PhastGel Blue R Coomassie stain (Pharmacia Biotech) for 10 min and then destained to visualize transfer efficiency. After washing, the membrane was incubated in rabbit anti-PARP bovine, primary antibody (Calbiochem, 15 μ l in 15 ml TBS), overnight at 4°C, washed for 30 min with TBS and then placed in anti-rabbit IgG secondary antibody conjugated to horseradish peroxidase (Sigma-Aldrich, 10 μ l in 15 ml of TBS) for 2 hr at 4°C, washed, and developed and visualized by 3,3'-diaminobenzidine tetrahydrochloride (DAB, Sigma-Aldrich).

Transmission Electron Microscopy

Washed embryos were fixed with fresh 3% electron microscopy grade glutaraldehyde (Sigma-Aldrich; v/v) for 3 hr at 4°C, rinsed with TBS, immersed in 1% osmium (Sigma-Aldrich) (v/v) for 1 hr at RT, and rinsed again. Embryos were then dehydrated in an acetone series, em-

bedded in Araldite, and cut by using a glass knife.

ACKNOWLEDGMENTS

This work was submitted by J.N. in partial fulfillment of the requirements for a Ph.D. J.N. was funded by the U.S. Department of Education.

REFERENCES

- Bollag DM, Rozycki MD, Edelstein SJ. 1996. Protein methods. New York: Wiley-Liss.
- Chan DW, Yager TD. 1998. Preparation and imaging of nuclear spreads from cells of the zebrafish embryo. Evidence for large degradation intermediates in apoptosis. *Chromosoma* 107: 39–60.
- Chandler JM, Cohen GM, MacFarlane M. 1998. Different subcellular distribution of caspase-3 and caspase-7 following Fas-induced apoptosis in mouse liver. *J Biol Chem* 273:10815–10818.
- Compton MM, Cidowski JA. 1992. Thymocyte apoptosis: a model of programmed cell death. *Trends Endocrinol Metab* 3:17–23.
- Darzynkiewicz Z, Bruno S, Del Bino G, Gorczyca W, Hotz MA, Lassota P, Traganos F. 1992. Features of apoptotic cells measured by flow cytometry. *Cytometry* 13:795–808.
- Darzynkiewicz Z, Li X, Gong J. 1994. Assays of cell viability: discrimination of cells dying by apoptosis. *Methods Cell Biol* 41:15–38.
- Enari M, Sakahira H, Yokoyama H, Okawa K, Iwamatsu A, Nagata S. 1998. A caspase-activated DNase that degrades DNA during apoptosis, and its inhibitor ICAD. *Nature* 391:43–50.
- Gavrieli Y, Sherman Y, Ben-Sasson SA. 1992. Identification of programmed cell death in situ via specific labeling of nuclear DNA fragmentation. *J Cell Biol* 119:493–501.
- Hensley C, Gautier J. 1997. A developmental timer that regulates apoptosis at the onset of gastrulation. *Mech Dev* 69:183–195.
- Hensley C, Gautier J. 1999. Developmental regulation of induced and programmed cell death in *Xenopus* embryos. In: Zakeri Z, Lockshin RA, Benitez-Bribiesca L, editors. Mechanisms of cell death. New York: New York Academy of Sciences. p 105–119.
- Ikegami R, Rivera-Bennetts AK, Brooker DL, Yager TD. 1997a. Effect of inhibitors of DNA replication on early zebrafish embryos: evidence for coordinate activation of multiple intrinsic cell-cycle checkpoints at the mid-blastula transition. *Zygote* 5:153–175.
- Ikegami R, Zhang J, Rivera-Bennetts AK, Yager TD. 1997b. Activation of the metaphase checkpoint and an apoptosis programme in the early zebrafish embryo, by treatment with the spindle-destabilising agent nocodazole. *Zygote* 5:329–350.
- Ikegami R, Hunter P, Yager TD. 1999. Developmental activation of the capability to undergo checkpoint-induced apoptosis in the early zebrafish embryo. *Dev Biol* 209:409–433.
- Kimmel CB, Ballard WW, Kimmel SR, Ullmann B, Schilling TF. 1995. Stages of embryonic development of the Zebrafish. *Dev Dyn* 203:253–310.
- Koopman G, Reutelingsperger CPM, Kuijten GAM, Keehnen RMJ, Pals ST, Van Oers MHJ. 1994. Annexin V for flow cytometric detection of phosphatidylserine expression on B cells undergoing apoptosis. *Blood* 84:1415–1420.
- Lazebnik YA, Kaufmann SH, Desnoyers S, Poirier GG, Earnshaw WC. 1994. Cleavage of poly(ADP-ribose) polymerase by a proteinase with properties like ICE. *Nature* 371:346–347.
- Levrud J-P, Adam M, Luciani M-F, Aubry L, Klein G, Golstein P. 2003. Cell death in *Dictyostelium*: assessing a genetic approach. In: Lockshin RA, Zakeri Z, editors. When cells die II. New York: Wiley-Liss.
- Lockshin RA, Zakeri Z. 2002. Caspase-independent cell deaths. *Curr Opin Cell Biol* 14:727–733.
- Lockshin RA, Zakeri Z. 2003. Introduction. In: Lockshin RA, Zakeri Z, editors. When cells die II. New York: Wiley-Liss.
- Martin SJ, Reutelingsperger CPM, McGahon AJ, Rader JA, Van Schie RCAA, LaFace DM, Green DR. 1995. Early redistribution of plasma membrane phosphatidylserine is a general feature of apoptosis regardless of the initiating stimulus: inhibition by overexpression of Bcl-2 and Abl. *J Exp Med* 182:1545–1556.
- Mirkes PE, Little SA. 2000. Cytochrome c release from mitochondria of early postimplantation murine embryos exposed to 4-hydroperoxycyclophosphamide, heat shock, and staurosporine. *Toxicol Appl Pharmacol* 162:197–206.
- Mizoguchi H, Kudo D, Shimizu Y, Hirota K, Kawai S, Hino A. 2000. Distribution of apoptosis-like cells in sea urchin early embryogenesis. *Zygote* 8(Suppl 1):S76.
- Nicholson DW, Ali A, Thornberry NA, Vaillancourt JP, Ding CK, Gallant M, Gareau Y, Griffin PR, Labelle M, Lazebnik YA, Munday NA, Raju SM, Smulson ME, Yamin T-T, Yu VL, Miller DK. 1995. Identification and inhibition of the ICE/CED-3 protease necessary for mammalian apoptosis. *Nature* 376: 37–43.
- Nicholson DW, Thornberry NA. 1997. Caspases: killer proteases. *Trends Biochem Sci* 22:299–306.
- Oberhammer F, Wilson JW, Dive C, Morris ID, Hickman JA, Wakeling AE, Walker PR, Sikorska M. 1993. Apoptotic death in epithelial cells: cleavage of DNA to 300 and/or 50 kb fragments prior to or in the absence of internucleosomal fragmentation. *EMBO J* 12: 3679–3684.
- Oliver FJ, de la Rubia G, Rolli V, Ruiz-Ruiz MC, De Murcia G, Murcia JM. 1998. Importance of poly(ADP-ribose) polymerase and its cleavage in apoptosis. Lesson from an uncleavable mutant. *J Biol Chem* 273:33533–33539.
- Oppenheim RW, Flavell RA, Vinsant S, Prevette D, Kuan CY, Rakic P. 2001. Programmed cell death of developing mammalian neurons after genetic deletion of caspases. *J Neurosci* 21:4752–4760.
- Trump BF, Berezsky IK, Osornio-Vargas AR. 1981. Cell death and the disease process. The role of calcium. In: Bowen ID, Lockshin RA, editors. Cell death in biology and pathology. London: Chapman and Hall. p 209–242.
- Westerfield M. 1998. The Zebrafish book. Available at: http://zfinfo.uoregon.edu/zf_info/zfbook/ (accessed 7 June 2004).
- Woo M, Hakem R, Soengas MS, Duncan GS, Shahinian A, Kagi D, Hakem A, McCurrach M, Khoo W, Kaufman SA, Senaldi G, Howard T, Lowe SW, Mak TW. 1998. Essential contribution of caspase 3/CPP32 to apoptosis and its associated nuclear changes. *Genes Dev* 12: 806–819.
- Wyllie AH. 1980. Glucocorticoid-induced thymocyte apoptosis is associated with endogenous endonuclease activation. *Nature* 284:555–556.
- Yabu T, Kishi S, Okazaki T, Yamashita M. 2001a. Characterization of zebrafish caspase-3 and induction of apoptosis through ceramide generation in fish fathead minnow tail bud cells and zebrafish embryo. *Biochem J* 360:39–47.
- Yabu T, Todoriki S, Yamashita M. 2001b. Stress-induced apoptosis by heat shock, UV and γ -ray irradiation in zebrafish embryos detected by increased caspase activity and whole-mount TUNEL staining. *Fish Sci* 67:333–340.
- Yager TD, Ikegami R, Rivera-Bennetts AK, Zhao C, Brooker D. 1997. High-resolution imaging at the cellular and subcellular levels in flattened whole mounts of early zebrafish embryos. *Biochem Cell Biol* 75:535–550.
- Yüce Ö, Sadler KC. 2001. Post-meiotic unfertilized starfish eggs die by apoptosis. *Dev Biol* 237:29–44.